AMPLITUDE AND PHASE ANALYSIS OF EARTH TIDE RECORDS ACROSS THE SAN ANDREAS FAULT

Robert L. Keller

REPORT

NAVAL POSTGRADUATE SCHOOL

Monterey, California

THESIS

AMPLITUDE AND PHASE ANALYSIS OF EARTH TIDE RECORDS ACROSS THE SAN ANDREAS FAULT

by

Robert L. Keller

March 1975

Thesis Advisor: D. R. Barr
R. H. Shudde

SECURITY CLASSIFICATION OF THIS PAGE (When Data Entered)

REPORT DOCUMENTATION PAGE

READ INSTRUCTIONS BEFORE COMPLETING FORM

1. REPORT NUMBER	2. GOVT ACCESSION NO. / 3. RECIPIENT'S CATALOG NUMBER
4. TITLE (and Subtitle): Amplitude and Phase Analysis of Earth Tide Records Across the San Andreas Fault	5. TYPE OF REPORT & PERIOD COVERED: Master's Thesis March 1975 / 6. PERFORMING ORG. REPORT NUMBER
7. AUTHOR(s): Robert L. Keller	8. CONTRACT OR GRANT NUMBER(s)
9. PERFORMING ORGANIZATION NAME AND ADDRESS: Naval Postgraduate School, Monterey, California 93940	10. PROGRAM ELEMENT, PROJECT, TASK AREA & WORK UNIT NUMBERS
11. CONTROLLING OFFICE NAME AND ADDRESS: Naval Postgraduate School, Monterey, California 93940	12. REPORT DATE: March 1975 / 13. NUMBER OF PAGES: 48
14. MONITORING AGENCY NAME & ADDRESS (if different from Controlling Office): Naval Postgraduate School, Monterey, California 93940	15. SECURITY CLASS. (of this report): Unclassified / 15a. DECLASSIFICATION/DOWNGRADING SCHEDULE

16. DISTRIBUTION STATEMENT (of this Report)

Approved for public release; distribution unlimited.

17. DISTRIBUTION STATEMENT (of the abstract entered in Block 20, if different from Report)

18. SUPPLEMENTARY NOTES

Thesis Advisors: Barr 2654
Shudde 2303

Autovon Ext. 479

19. KEY WORDS (Continue on reverse side if necessary and identify by block number)

20. ABSTRACT (Continue on reverse side if necessary and identify by block number)

This study establishes the existence of damping structural properties in the San Andreas Fault zone through an input model of surface loading. Any changes in the density, mass or bulk elastic properties of a fault zone will not only produce a change in the gravity field of the earth, but also a change in the earth's response to the tidal field generated by the moon. Knowledge of these changes is important to engineering constructions, pre-programmed defense systems, etc. To adequately measure these

DD FORM 1 JAN 73 1473 EDITION OF 1 NOV 65 IS OBSOLETE
S/N 0102-014-6601

SECURITY CLASSIFICATION OF THIS PAGE (When Data Entered)

responses, sites on opposite sides of the San Andreas Fault zone were selected and tidal gravity was continuously measured for finite periods of time. The Pacific Ocean and its very low frequency lunar portion of the ocean load spectrum was used as a driving function to compare observed data with theoretically generated data for the same sites. A least squares criteria was used to fit the observed and theoretical data to the nine most important spectral lines and to obtain the phase and amplitude for each line at both sites. Utilizing the most stable lines to compare values, a significant drop (about 10%) in both phase and amplitude occurred between the two sites. The anomalous decrease in both areas of analysis discloses a structural damping in the San Andreas Fault zone.

Amplitude and Phase Analysis of Earth Tide Records Across the San Andreas Fault

by

Robert L. Keller
Captain, United States Army
B.S., United States Military Academy, 1968

Submitted in partial fulfillment of the
requirements for the degree of

MASTER OF SCIENCE IN OPERATIONS RESEARCH

from the

NAVAL POSTGRADUATE SCHOOL
March 1975

ABSTRACT

This study establishes the existence of damping structural properties in the San Andreas Fault zone through an input model of surface loading. Any changes in the density, mass or bulk elastic properties of a fault zone will not only produce a change in the gravity field of the earth, but also a change in the earth's response to the tidal field generated by the moon. Knowledge of these changes is important to engineering constructions, pre-programmed defense systems, etc. To adequately measure these responses, sites on opposite sides of the San Andreas Fault zone were selected and tidal gravity was continuously measured for finite periods of time. The Pacific Ocean and its very low frequency lunar portion of the ocean load spectrum was used as a driving function to compare observed data with theoretically generated data for the same sites. A least squares criteria was used to fit the observed and theoretical data to the nine most important spectral lines and to obtain the phase and amplitude for each line at both sites. Utilizing the most stable lines to compare values, a significant drop (about 10%) in both phase and amplitude occurred between the two sites. The anomalous decrease in both areas of analysis discloses a structural damping in the San Andreas Fault zone.

TABLE OF CONTENTS

LIST OF TABLES

LIST OF FIGURES

I. INTRODUCTION

A. STATEMENT OF THE PROBLEM

The combined gravitational fields of the moon and the sun acting on the solid earth are sufficient to displace its surface on the order of 20 cm. semi-daily [1]. Unfortunately, this direct forcing function is so broad in its areal extent (i.e., several thousand kilometers) that it cannot reasonably be used to study responses of small crustal structures (such as fault zones) [2] which are on the order of a few kilometers in width and depth. However, the response of the ocean to the lunar-solar gravitational field (on the order of meters) constitutes a sufficiently energetic forcing function such that under certain conditions dynamic properties of crustal structures can be studied.

The conditions under which the ocean can effectively be used as a forcing function to study the properties of a shallow structure are defined as:

1. The distance between the edge of the ocean load and the fault structure should not exceed the smallest dimension of the fault zone by one order of magnitude [3];

2. Noise response in the earth tide records obtained during this experiment must be kept to a minimum. Minimizing noise response is achieved by using parts of the ocean tidal spectrum which are both stationary and relatively unaffected by meteorological influences.

The two lines chosen for amplitude and phase analysis in this study are the principal lunar diurnal O_1 and the principal lunar semi-diurnal M_2 lines which are the most energetic in the theoretical tidal spectrum and are the most removed from possible contamination due to meteorologically induced noises.

Earthquake prediction research explores the causes of earthquakes from two points of view: (1) failure brought about by an external increase of shear stress which exceeds the shear modulus of the fault; (2) failure brought about when the internal properties of the fault change (coefficient of shear) until they are reduced below that of the external shear being applied.

In this study responses to tidal gravity were measured at two points on either side of the San Andreas Fault. Tidal gravity is a vertical measure of the acceleration due to gravity. The value of gravity is on the order of 10^3cm/sec/-sec or 10^3 gal. Resolution on the order of 10^{-6} gal is achieved with the instruments used (described below) giving results accurate to one part in a 10^9. The distance between the two stations (about 5 kilometers) is small compared to the distance to the edge of the ocean load (Pacific Ocean, about 30 km). The amplitude and phase of the two measured lunar tidal constituents (O_1 and M_2) were compared with the amplitude and phase of the same two lines derived from an analysis of the theoretical tidal gravity calculated at each

of the two sites for identical periods of time. The difference in the observed phases between the sites was compared with the difference in theoretical phases between the sites and a 10% change in the means was observed.

This result suggests that the principal source for the phase difference between the observed and theoretical values at both sites is due to the response of these sites to ocean tidal loading at the same frequency. However, a 10% deviation of the difference between these two sites from the mean is significantly large and is not due to a simple shift of a few kilometers further away from the coastline. Instead, the anomalously large difference in the comparison is explained by the fact that the stations are not just separated by a few kilometers but that they lie on opposite sides of a weakness in the earth's crust. The absolute difference between the most inland station and the other is a lag of about three degrees at the M_2 frequency. This is interprted primarily as a viscoelastic response of the fault zone to ocean tidal loading. The inland edge of the San Andreas Fault reaches it peak amplitude of ocean tidal response approximately 1/10 hour after the peak response of the ocean side of the fault.

While this study did not attempt to directly calculate any geological strength parameters, it did suggest the existence of a crustal weakness with viscoelastic properties that strongly dampen the M_2 line of the ocean tidal loading.

B. BACKGROUND

There exists in any multi-body system a measurable gravitational potential due to the attacting fields of the many masses (or bodies) present. Since all bodies have motion relative to all others in a system, the potential fields fluctuate with time. On the earth, only the sun and the moon contain sufficiently large quantities of mass at a close enough distance to significantly affect tidal variations or time fluctuations in the potential field.

The effects from the sun and the moon generate earth tides in a similar manner to their production of ocean tides. Unfortunately, the study of earth tides is complicated by the presence of oceans which also cause changes in earth tides. Although quite small, ocean loading effects on the earth tides have been detected in measurements as far inland as mid-continent in the United States [4]. The mass of the oceans complicates measurements of the earth tides in the same ways as external masses (the sun and moon) plus (1) the loading effect due to water (additional mass) and (2) deformation of the earth due to the redistribution of ocean waters as the water more freely fluctuates.

The combination of effects of the sun, moon and oceans over time results in a continuous change in the earth's gravity. The gravitational force at any given point in time and space can be broken into two components, one normal to the plane tangent to the earth's surface and one in the

plane tangent to the surface. This study will concentrate on the former component called tidal gravity.

Past geological and seismological studies have examined the bulk elastic properties of the whole earth and the distribution of these properties in the core and the mantle. Few studies have narrowed their objective to examining the bulk elastic properties of only the crust of the earth and in a relatively small area. Seismic studies show that the San Andreas Fault zone has brittle properties to a depth of only ten kilometers, which is neither the bottom of the fault nor the bottom of the continental plate [5]. It is approximately one-third of the depth of the plate. Authors of these studies quite often generalize their results to large area averages and tend to overshadow the relatively small area of a shallow fault zone in the final analysis [2]. The seismic studies and their related high frequencies (from earthquakes) also do not allow determination of anelastic responses, but very low frequency studies such as those resulting from ocean loading should disclose any anelastic properties present.

This study is a portion of a larger project, (headed by Dr. M. D. Wood) at the National Center for Earthquake Research (NCER), to establish that the response of the earth to tidal loading is significantly perturbed by the San Andreas Fault and also to determine through spatial and temporal means the bulk properties of the fault zone.

There are two possible sources of error in analyzing these data that should be noted. First, due to many constraints, the three experiments in this study were performed sequentially instead of simultaneously. Second, the San Francisco Bay, due to its size and its proximity to the sites, will affect the values measured in the experiment. The effects of these errors are assumed to be relatively small, but their exact effects are undetermined.

II. DATA ACQUISITION AND PROCESSING

A. LOCATION SELECTION

The locations selected for the two main sites for this analysis were obtained from a threefold criterion. First, it was desired to ensure that the two sites were on opposite sides of the San Andreas Fault zone and nearly equidistant from the fault region. This was necessary in order to obtain spatial analysis of the tidal wave as it passed from one site to the other by traversing through the fault region. Second, the sites were desired to be on a line nearly perpendicular to the coastline. Third was the availability of suitable sites. It was imperative that the physical location of each instrument be based on a very sturdy foundation, ideally on deep lying rock, to minimize noise. To further eliminate noises (in the form of other energies such as wind, temperature fluctuation, surface vibrations, etc.) it was desirable to place each recording instrument below the surface of the earth. Time and financial restrictions forced a compromise of this desire to a level, surface (or very shallow) base that was protected from as many of the other noise-producing sources as possible. In addition to these restrictions, the security of the expensive recording instruments became a major concern. The instruments could not be left in the open where vandals or sightseers might tamper with them. It was also desired to have daily time marks entered on each record, generating the requirement for

someone to be present at the site each day to perform this task. Appropriate sites with the necessary attendance requirements were located [Figure 1]. One recording instrument was in a basement vault on a base on concrete poured on solid rock (Block experiment); another was in a separate garage on a concrete base poured on rock (Rose experiment). Both properties were private and actual instrument locations were secure. The third site was located in the NCER Building in Menlo Park on a concrete floor (NCER experiment).

B. EARTH TIDE RECORDINGS

All the earth tide recordings were taken from LaCoste-Romberg Earth Tide Gravity Meter type instruments [1] on paper strip charts [Figure 2]. These were recorded from NCER owned instruments run by 120v AC with 12v automobile batteries as a back-up.

To allow future adjustments for inaccuracies in chart speed, stretching or shrinking, etc., daily time marks were mechanically entered on each chart and labeled. Chart speed for each experiment was two inches per hour with a displacement of one inch equal to 30 μgal. Each experiment was attempted to run at least thirty days to give a large enough sample for adequate analysis [6].

C. DATA PROCESSING

The strip charts were digitized onto magnetic tape by use of a Calma 302 digitizer. The cross-hair cursor moved

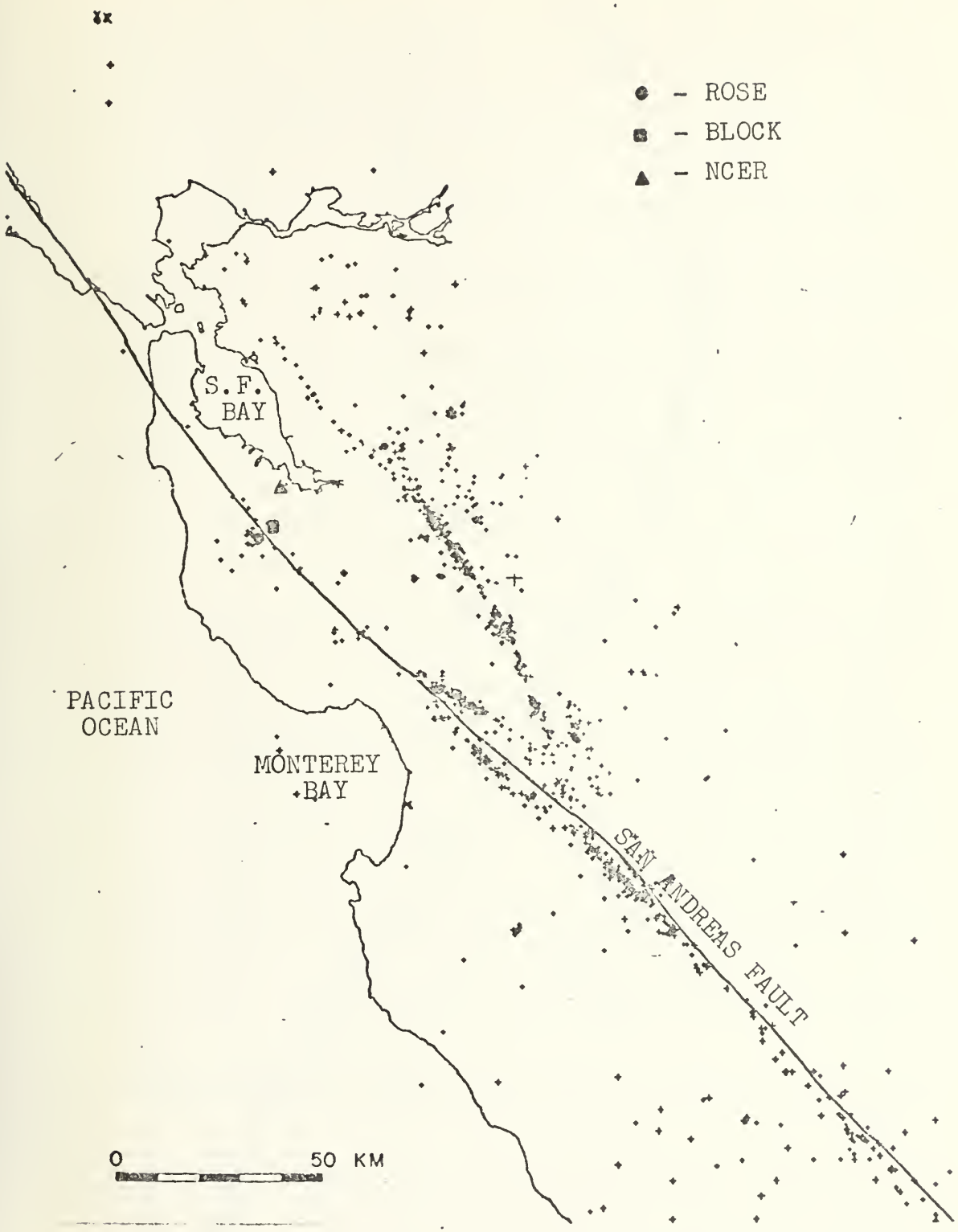

Figure 1. Test Site Locations.

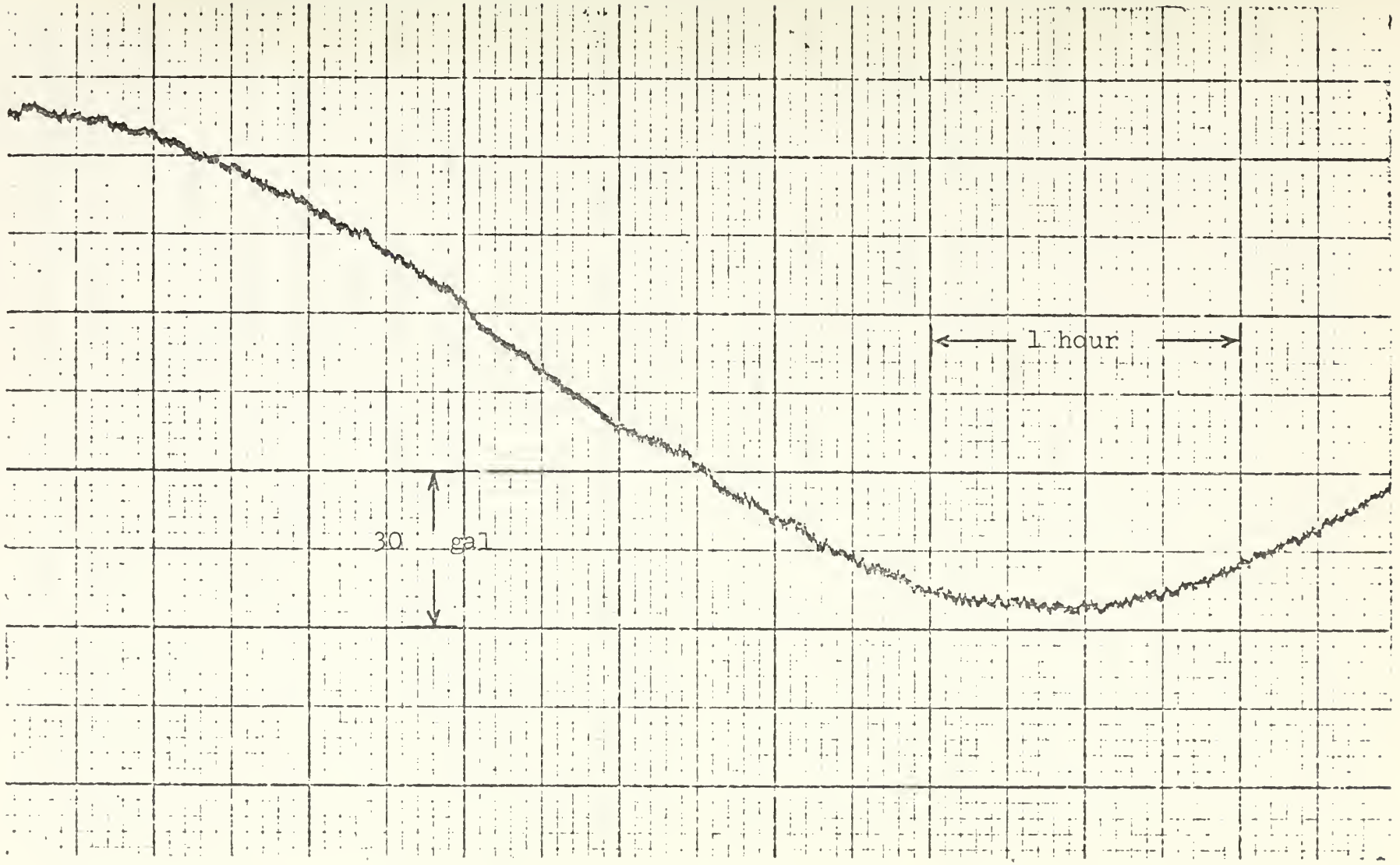

Figure 2. Raw Data of Earth Tide from Rose Experiment.

vertically or horizontally as desired across the strip chart taking discrete samples every .01 inches and recording the readings. A special indication was noted at each daily time mark entered on the chart by monitoring personnel, and the time and date were recorded by the person performing the digitization. The digital tape data was later corrected for chart stretching, shrinkage, etc., by proportionally distributing the actual recorded values between time marks to the correct number of .01 inch increments (.01 inch corresponds to 18 seconds of time) required between the daily time marks. This localized physical errors between time marks (usually every 24 hours) and minimized accumulation of error.

The digitized data consisted of readings based on a continuous time record. These data were then processed with a computer program (designed by M. D. Wood and P. A. Marshall [7] from the National Center for Earthquake Research (NCER) and modified by M. D. Wood and R. L. Keller for use in this study) which decimated the sample interval from .01 inches to hourly values taken on the hour.

Sampling theory requires a sample interval at least twice as often as the highest expected frequency. Implicit in this is the assumption that the recorded data be of a reasonable duration of time. A reasonable time duration is proportional to the reciprocal of the smallest difference between any two frequencies expected in the data [6]. Since only

nine lines of the 80-plus theoretical lines are used, it can be calculated that at least one month of data is necessary for a 1% resolution of tidal data [6]. The smallest frequency line used in this study is the M_4 with a frequency of less than 4 cycles/day, requiring at least 8 samples per day. By oversampling, the resolution remains well within 1%.

III. LEAST SQUARES ANALYSIS

A. AMPLITUDE ANALYSIS

The observed tidal gravity records were fit with a least squares computer program to the nine theoretical lines of the earth tide spectrum (explained in Appendix A). The computer program (designed by M. D. Wood [6] and modified by M. D. Wood and N. E. King of NCER and R. L. Keller) performs a regression of the data to fit both an $n^{\underline{th}}$ polynomial and a sine wave function simultaneously. The results give the amplitudes and phases of the nine lines mentioned above.

It is a well established fact that the principal lunar semi-diurnal M_2 and the principal lunar diurnal O_1 lines of the earth tide frequency spectrum are the most invariant of all the tidal lines [1], [6], [8]. Of these two, the M_2 line has proven to be less variant from its theoretical value than the other lines in previous studies conducted in this region [6], [7], [8] and was thus used as a normalizing factor for all of the spectral lines. The normalized amplitudes were computed using the following formula:

$$A_i^r = A_i/A_{M2}$$

where A_i^r is the (dimensionless) relative amplitude, A_i is the amplitude of the constituent line being normalized, and A_{M2} is the amplitude of the M_2 line. This normalizing process results in dimensionless values, facilitating comparison between observed and theoretical results.

The normalizing of the amplitudes of the selected lines in the earth tide spectrum was conducted for both the theoretical data [Table III] and for the observed data [Table IV]. Visual displays of these data are given in Figure 7 and Figure 8.

Taking the expected amplitude (theoretical) of each constituent line for each of the sites and subtracting the corresponding observed amplitude, the amplitude differences are obtained [Table I]. Differences can be expected due to forcing nine lines of a frequency spectrum to absorb what is acknowledged to consist of at least 89 lines and also due to other non-tidal factors such as seasonal noise, extreme weather conditions, etc. These differences should remain about constant between sites (resulting in low values in the last column) and would indicate a high stability of a constituent line. The last column of Table I shows a standard deviation of about 5% for the O_1 line from its average theoretical mean. This indicates that the O_1 line could be predicted to have a measured (observed) value with a standard deviation equal to about 5% of the theoretical value of the amplitude.

The normalizing of the amplitudes of the selected lines in the earth tide spectrum was conducted for both the theoretical data [Table II] and for the observed data [Table III]. Visual displays of these data are given in Figure 3 and Figure 4. These tables and figures are presented here to facilitate comparison of the results obtained in this study to those of other completed studies [6], [7], [8] making use of similar types of displays.

A relative gravimetric factor G_i^r can be computed by the following formula:

$$G_i^r = A_i^r \text{ (experimental)}/A_i^r \text{ (theoretical)}$$

where the A_i^r are described above. Using the two most stable lines to establish a comparative base, we compute:

$$G^r(O_1/M_2) = A^r(O_1/M_2)(\text{experimental})/A^r(O_1/M_2)(\text{theoretical})$$

Theoretically, this ratio should equal to 1.00, but with other dynamic considerations a 1% variation [9] is accepted. Ten world-wide stations studied by Harrison and others [10] resulted in an average value of :

$$G^r(O_1/M_2) = 0.989 \pm 0.035.$$

Four stations in the San Francisco Bay area analyzed by Wood [6] gave an average value of:

$$G^r(O_1/M_2) = 0.938 \pm 0.026.$$

The average value obtained by the three stations in this study gave:

$$G^r(O_1/M_2) = 1.051 \pm 0.061.$$

These values should not be different, regardless of location, yet this study and that by Wood indicate values about 4% to 5% outside of the accepted range. Both of these studies were conducted on the West Coast near the San Francisco Bay Region and could indicate a local disparity from areas with thicker crustal depths (The California coastal regions are known to have a much thinner crustal depth than most other continental areas). However, no conclusion is drawn from this study other than to mention that this disparity should not exist.

B. PHASE ANALYSIS

The observed tidal gravity records were simultaneously fit in the least squares program (described in the previous section) to the nine theoretical waves of the earth tide spectrum to estimate the phase of each constituent line. The values for both theoretical and observed phases for the M_2 lines are given in Table IV. All charts were maintained in reference to Greenwich Time (GMT) except for the Rose site which was marked in local daylight time. A seven hour difference existed between these base reference times and the phase was appropriately advanced for this discrepancy.

The results show a phase difference between the theoretical and observed M_2 line at both the Rose site and the Block site.

TABLE I. RELATIVE EARTH TIDE FACTORS - COMPARATIVE RESULTS

Tide Line	Amplitude Differences			Mean Difference	Standard Deviation	Standard Deviation (% of Mean)*
	Rose	Block	NCER			
M2	0.0000	0.0000	0.0000	0.0000	0.0000	0.0000
N2	0.0309	0.0413	-0.0004	0.0239	0.0217	10.8068
S2	-0.4972	-0.0292	-0.0125	-0.1796	0.2751	58.5319
K2	-0.5428	-0.2540	0.1821	-0.2049	0.3649	160.8906
P1	-0.5492	-0.1431	-0.0681	-0.2535	0.3660	94.2085
K1	-0.1145	-0.3074	-0.0128	-0.1449	0.2357	29.6739
O1	-0.0560	0.0060	-0.0440	-0.0313	0.0328	5.3195
Q1	-0.0008	-0.0872	-0.0140	-0.0335	0.0471	40.4639
M4	-0.030690	-0.010657	-0.003343	-0.011563	0.00871	380.0174

*Standard deviation as a percentage of the average theoretical amplitudes.

TABLE II. RELATIVE EARTH TIDE AMPLITUDE FACTORS - THEORETICAL

Tide Line	Relative Amplitudes			Mean Amplitude	Standard Deviation	Standard Deviation (% of Mean)
	Rose	Block	NCER			
M2	1.0000	1.0000	1.0000	1.0000	0.0000	0.0000
N2	0.1857	0.2171	0.1997	0.2008	0.0157	7.8187
S2	0.5688	0.5022	0.3390	0.4700	0.1183	25.1489
K2	0.2350	0.2345	0.2110	0.2268	0.0137	6.0406
P1	0.3323.	0.5638	0.2694	0.3885	0.0227	5.8430
K1	0.8150	0.7276	0.8404	0.7943	0.0593	7.4657
O1	0.5984	0.6116	0.6399	0.6166	0.0212	3.4382
Q1	0.1090	0.1071	0.1330	0.1164	0.0144	12.3711
M4	0.002720	0.001703	0.002453	0.002292	0.000527	22.9930

TABLE III. RELATIVE EARTH TIDE AMPLITUDE FACTORS - OBSERVED

Tide Line	Relative Amplitudes			Mean Amplitude	Standard Deviation	Standard Deviation (% of Mean)
	Rose	Black	NCER			
M2	1.0000	1.0000	1.0000	1.0000	0.0000	0.0000
N2	0.1548	0.1758	0.2001	0.1769	0.0226	12.7756
S2	1.0660	0.5314	0.3515	0.6496	0.3716	57.2044
K2	0.7778	0.4885	0.0289	0.4317	0.3777	87.4913
P1	0.8815	0.7069	0.3375	0.6420	0.2777	43.2554
K1	0.7005	1.0350	0.8532	0.8629	0.1675	19.4113
O1	0.6544	0.6056	0.6839	0.6480	0.0395	6.0957
Q1	0.1082	0.1943	0.1470	0.1498	0.0431	28.7717
M4	0.023410	0.012360	0.005796	0.013860	0.008900	64.2136

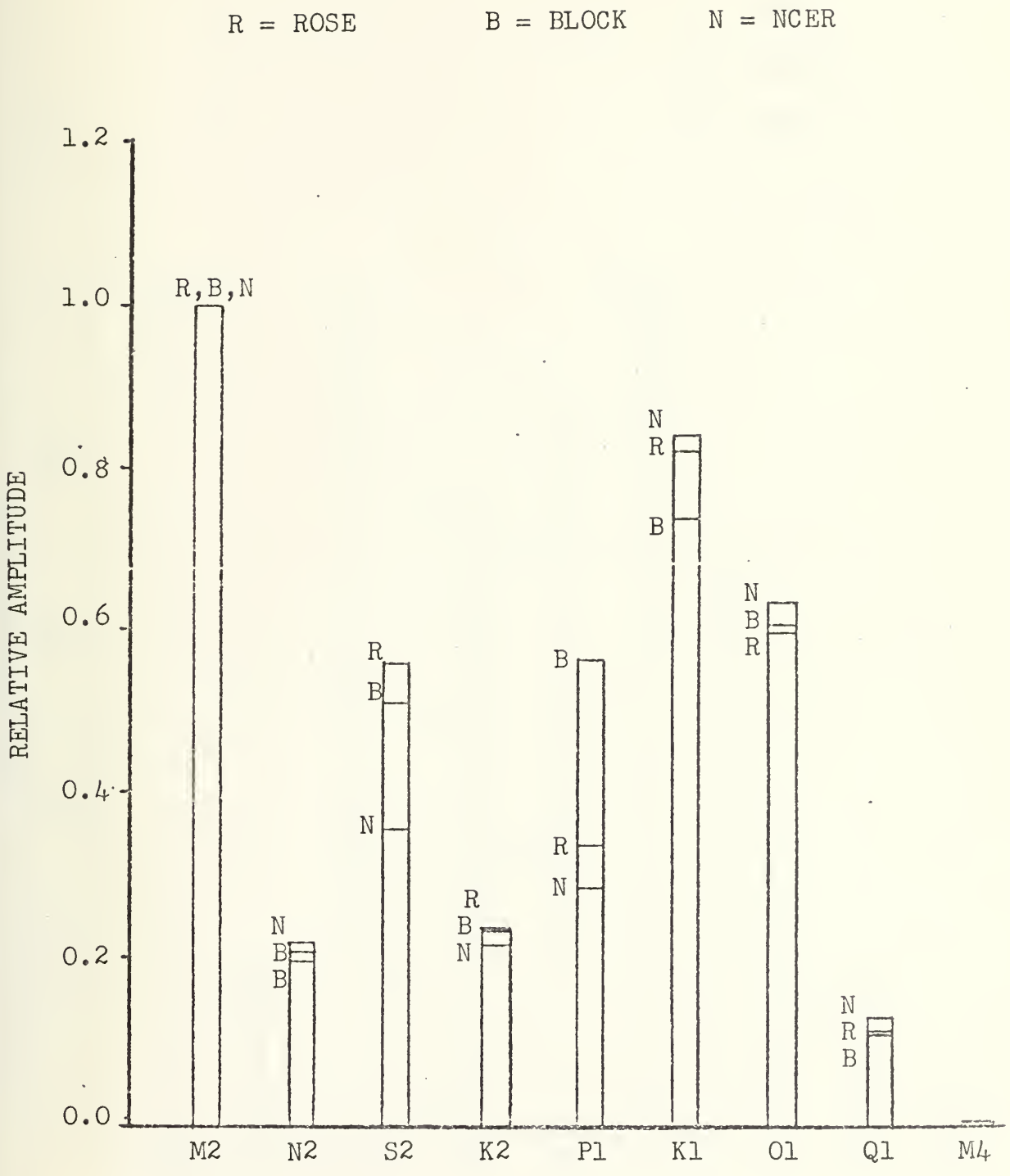

Figure 3. Composite Theoretical Amplitude Histogram Normalized by M_2 Component

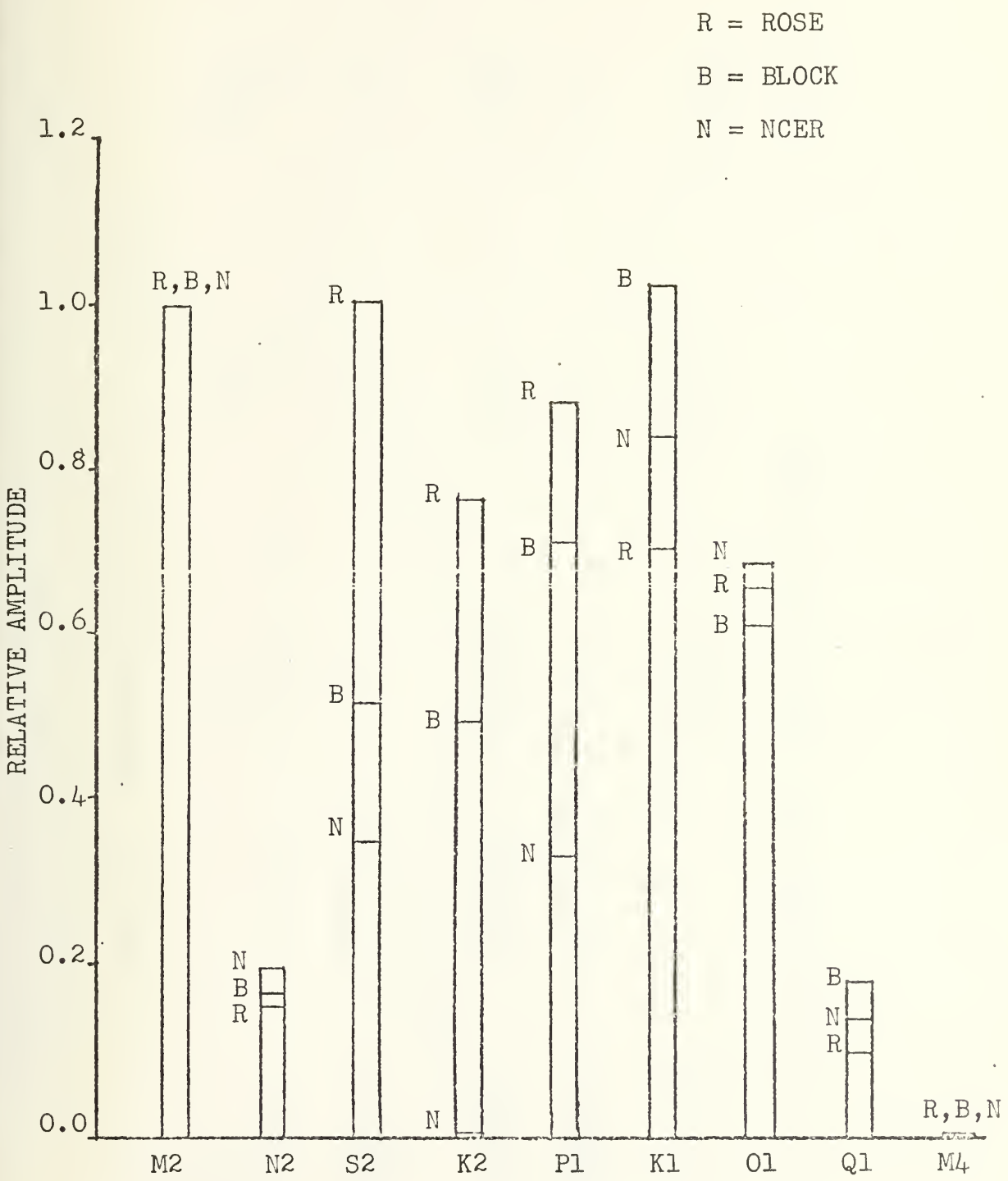

Figure 4. Composite Observed Amplitude Histogram, Normalized by M_2 Component.

TABLE IV. RELATIVE EARTH TIDE PHASE COMPARISONS

Site		Rose	Block	NCER
Absolute	Observed	1.584	.7365	.2256
Phase (Radians) (θ)	Theoretical	1.503	.2342	.5845
Absolute	Observed	112.126*	42.198	12.926
Phase (Degrees) ( )	Theoretical	86.114	13.419	33.489
Difference		26.012	28.779	-20.563

*Value corrected from local daylight time to GMT.

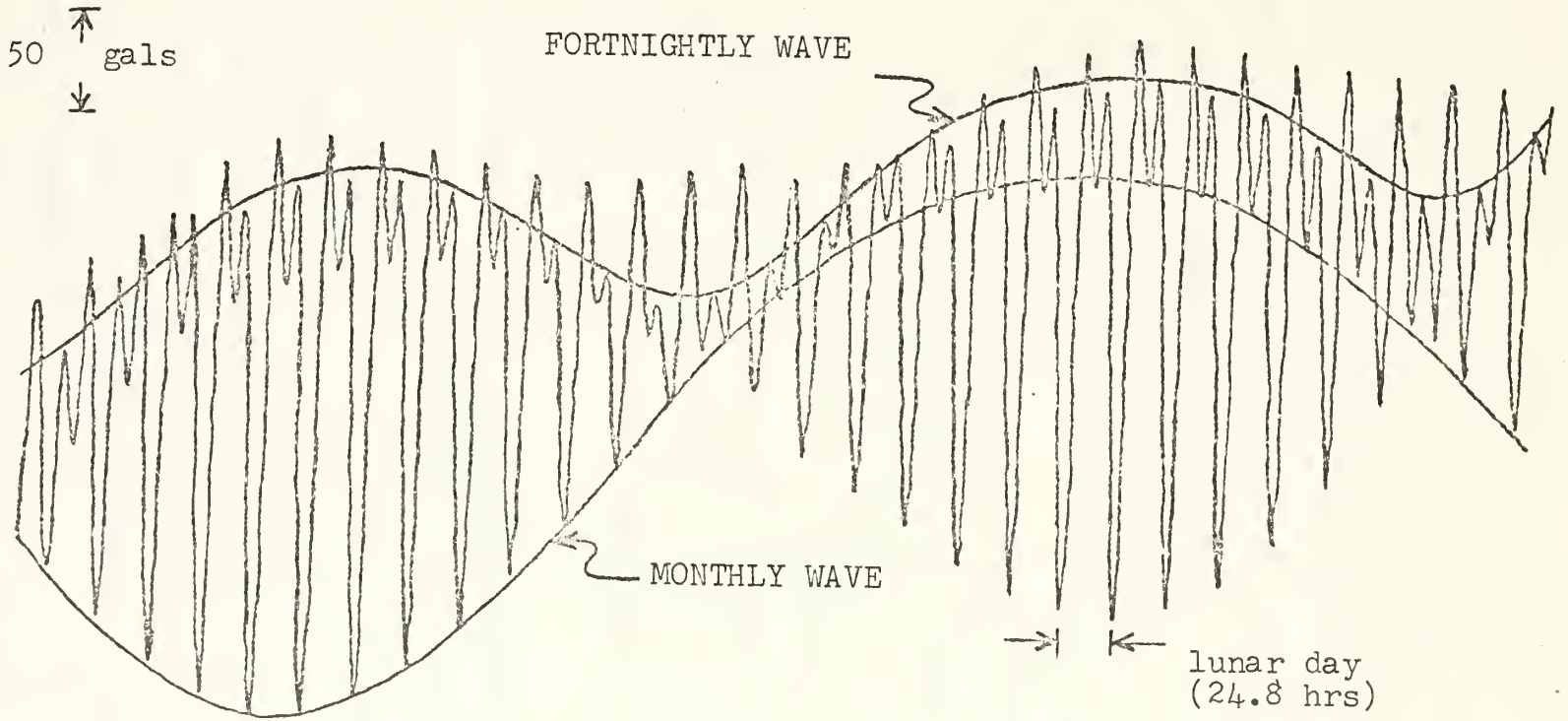

Figure 5. Tidal Gravity Record illustrating Monthly and Fortnightly Waves due to varying lunar orbital ellipticity and declination respectively. (Adopted from Wood [7])

IV. RESULTS

The average value of $G^r(O_1/M_2)$ was much higher than those produced by the experiments done by Harrison and others [10] and Wood [7]. As noted above, no explanation for this has to date been found. The relative gravimetric factor showed a downward change between the two sites. It decreased by more than 0.1, or about a 10% drop in value.

In the examination of the two most stable lines in the earth tide spectrum, the value of the O_1/M_2 (the normalized amplitude of the O_1 constituent line) decreased from the Rose to the Block station by a value of .0488 which is about a $7\frac{1}{2}\%$ decrease between the two sites. Theoretically, the normalized O_1 line amplitude should not show much change in value, specifically across a distance of 5 km. From the values in Table II, it can be shown that about a 2% increase should have occurred.

There also exists a phase difference between the theoretical and observed data at each site. The observed and theoretical lines should all be in phase with each other. Allowing for small variations due to noise and tectonic interferences prior to the arrival of the M_2 line at the Rose site (again the most stable line is selected for comparison), there may exist a phase difference between theoretical and observed lines. Between the Rose and Block sites, however, this difference should remain constant. In fact, it does not; it changes by more than $2\frac{1}{2}$ degrees. This change is a

decrease in phase difference, or a lag, of about $9\frac{1}{2}\%$ between the two sites. Physically interpreted, this is a time delay of about 1/10 hour for peak amplitude of the M_2 wave to travel from the Rose to the Block site.

V. CONCLUSIONS AND RECOMMENDATIONS

With the evidence advanced in this study, it appears that some disturbing factor has caused a large percentage decrease in tidal amplitude and phase between the Rose and the Block sites. These percentage changes are much too great to be explained by the 5 km. distance between the sites. The fact that the San Andreas Fault is located between these two sites leads one to suspect that drastic changes in earth tides between the two sites might be due to the fault region and its different structural properties from surrounding area properties.

Assuming that the fault region is responsible for these tidal changes, it is possible to calculate the approximate strength parameters of the geological structure of the fault region itself through a more detailed geological study of sites across the fault.

Since this experiment was limited in time, money, equipment, available sites, etc., it cannot provide absolute proof that the fault region is responsible for the observed changes. The study provides evidence that the fault might be reason for the observed changes. It is recommended that further investigations of a similar nature be conducted at sites void of an inland bay to verify the results of this study. These future studies could also be set up to simultaneously examine the specific geological properties exhibited by the fault region in each area of study.

APPENDIX A

THEORY OF EARTH TIDES

A study of the earth tide curve shown in Figure 5 reveals the presence of at least two frequency components of the earth tide spectrum. Identified in this figure are the diurnal frequency with a period of approximately 28 days and the semi-diurnal frequency with an approximate 14 day period. A Fourier analysis of a record such as this reveals that there exist many constituent waves that combine to give us the wave form. Analysis of longer records would reveal semi-annual, annual, and even longer period waves which correspond to motions of the sun and moon in relation to the earth.

When the complex relationships between the moon (and sun) of a rigid earth are considered, the constituent waves (lines in the spectrum) derived via the Fourier analysis become meaningful. Let us examine a fictitious model [6], [8] in which the moon is orbiting about the earth in the plane of the earth's equator at a constant distance with a constant velocity equal to the mean distance and velocity of the actual moon. The earth is also revolving on its axis once every 24 hours and this motion plus the moon's gravitational attraction on the earth's surface produces a tide with a period equal to a lunar half-day and is described by the M_2 principal lunar semi-diurnal line, the most energetic of the semi-diurnal lines. In similar fashion, the S_2 principal

solar semi-diurnal line is produced by a fictitious sun in a circular orbit at a constant velocity and distance.

If the moon's declination in its orbit (above or below the plane of the earth's equator) is now added to our simple model, the distance between the moon and an observation point on the earth varies with time, but in a different manner than the simpler model. In the simple model, the distance variation with time was due only to the observer's position and the lunar position in the equatorial plane. Now a declination distance away from the equatorial plane also varies with time as well as the consideration for the earlier model, adding another variable to be considered in the distance variation between the moon and an observation point on earth. For observation points on the equator, the effects of the lunar orbit in the northern and southern hemisphere are equal in magnitude. For non-equatorial observers, the amplitude of the two diurnal maxima would vary in time with the changing distance from the observation point to the moon. This is referred to as the diurnal inequality. The cyclical motion of the moon's declination causes a fortnightly modulation of the earth tides.

Adding the ellipticity of the moon's orbit to our model now leads to the cyclical changes in the distance from the moon to the earth and causes modulation of both the amplitudes and phases of all the above effects.

Associating a theoretical wave with each of the motions of the moon does not complete an explanation of the earth tide spectrum. Secondary waves are apparent due to the beat frequencies of the principal tide waves. These beat frequencies are obtained from the sum and difference frequencies of the two principal waves. When the difference in the lunar and solar principal semi-diurnal waves (M_2 and S_2) is taken, a fortnightly modulation occurs at the beat frequency. The lunar elliptic semi-diurnal wave, N_2, and the M_2 wave combine for a beat frequency to form a modulation with a monthly period that is associated with the eccentricity of the lunar orbit. The K_2 luni-solar semi-diurnal declinational wave is composed of lunar and solar components which are analytically inseparable, as is the K_1 luni-solar diurnal declination wave.

Further beat frequencies exist which yield waves derived in a similar fashion. Table I lists the principal theoretical tidal waves of the earth tide spectrum which are of importance to this study. The amplitude of each of these waves is dependent on latitude and varies with time.

APPENDIX B

THEORETICAL TIDE GENERATION

The gravitational potential at some point P on the surface of the earth [Figure 6] due to another mass (moon or sun) can be expressed as [6], [11], [12]:

$$W = GM\frac{r^2}{R^3}\sum_{n=o}^{\infty}\left(\frac{r}{R}\right)^n \cdot P_n(z) = \sum_{n=o}^{\infty} W_n$$

where
- G is a gravitational constant
- M is the external mass
- r is the radius of the earth
- R is the absolute distance from the earth to the external mass
- $P_n(z)$ is the Legendre polynomial
- z is the angular position of the external mass relative to the zenith of point P
- P is a point on the earth's surface.

Expanding the terms in the summation above necessitates the calculation of the Legendre polynomials. The first few terms of the Legendre polynomials are [12]:

$$P_o(z) = 1$$
$$P_1(z) = z$$
$$P_2(z) = \tfrac{1}{2}(3z^2-1)$$
$$P_3(z) = \tfrac{1}{2}(5z^3-3\ )$$
$$P_4(z) = 1/8(35z^4-30z^2+3)$$

Examining these results it is seen that the first term, $W_o=GM(1/R)$, is constant and has no effect on changing the gravitational potential. The second term, $W_1=GM(r/R^2)\cos(z)$, uniformly affects all points on the surface of the earth and has no effect on changing the potential. The third term (and all

remaining terms) affect the tidal potential and are all candidates for significant effects in the summation. The r/R term in the summation is approximately 1/60 for the moon and 1/2400 for the sun and after n=3 accounts for less than 2% of the previous term. Thus, the gravitational potential can be reduced to the simple expression:

$$W_2 = GM\frac{r^2}{R^3} P_2(z) = GM\frac{r^2}{R^3} \tfrac{1}{2}(3\cos^2(z)-1).$$

To express z in terms of fundamental angular parameters of position, spherical trigonometry is applied where:

δ = declination of external mass M

t = hour angle of point P

α = zenith angle of external mass at point P

φ = latitude of P

λ = longitude of P

z = polar angle of external mass M

Using the trigonometric relation:

$$\cos(\alpha) = \cos(\theta)\cos(z) + \sin(\theta)\sin(z)\cos(t)$$

and $\cos(\theta) = \sin(\varphi)$, $\sin(\theta) = \cos(\varphi)$

$\cos(z) = \sin(\delta)$, $\sin(z) = \cos(\delta)$

the gravitational potential becomes

$$W_2 = GM\frac{r^2}{R^3} \tfrac{1}{2} (3[\sin(\varphi)\sin(\delta) + \cos(\varphi)\cos(\delta)\cos(t)]^2-1)$$

and simplifies to

$$W_2 = 3K(\sin^2(\varphi)-1/3)(\sin^2(\delta)-1/3) + K(\sin(2\varphi)\sin(2\delta)\cos(t)) + K(\cos^2(\varphi)\cos^2(\delta)\cos(2t))$$

where $K = 3/4GM\frac{r^2}{R^3}$

This equation is shown in Figure 7.

Using the moon as an example, the first term in this expression contains the variable δ (φ is constant for a given point P), namely $\sin^2(\delta)$, which is an even function varying as the declination of the mass M traverses from its maximum positive value to its maximum negative value and back each month. The functional value stays positive (since $\sin^2(\delta)$ is an even function) and the frequency of the first term becomes two cycles per month and is called the fortnightly wave. The second term varies with δ and t, but δ completes a cycle in one month while t has a period of about one day. Therefore, this term has a frequency of one cycle per lunar day and is called the diurnal wave. Similarly, the third term, with a frequency of two cycles per lunar day, is called the semi-diurnal wave.

A similar situation occurs with the sun as the external mass, and the sum of the results from the moon and the sun yields the terms of the tidal potential. The remainder of the tidal potential spectrum consists of the higher ordered terms and combined lunar-solar terms neglected in this analysis. For the purposes of this study the nine waves described in Table V are sufficient since they contain more than 90% of the effects of the 89 theoretical lines.

In the generation of the theoretical earth tides for this study, J. C. Harrison's program [13] was used. In the development of his model for generating earth tides, Harrison

uses W_2 for the moon (as described above) and W_2 for the sun and also includes W_3 for the moon to achieve greater precision in his results.

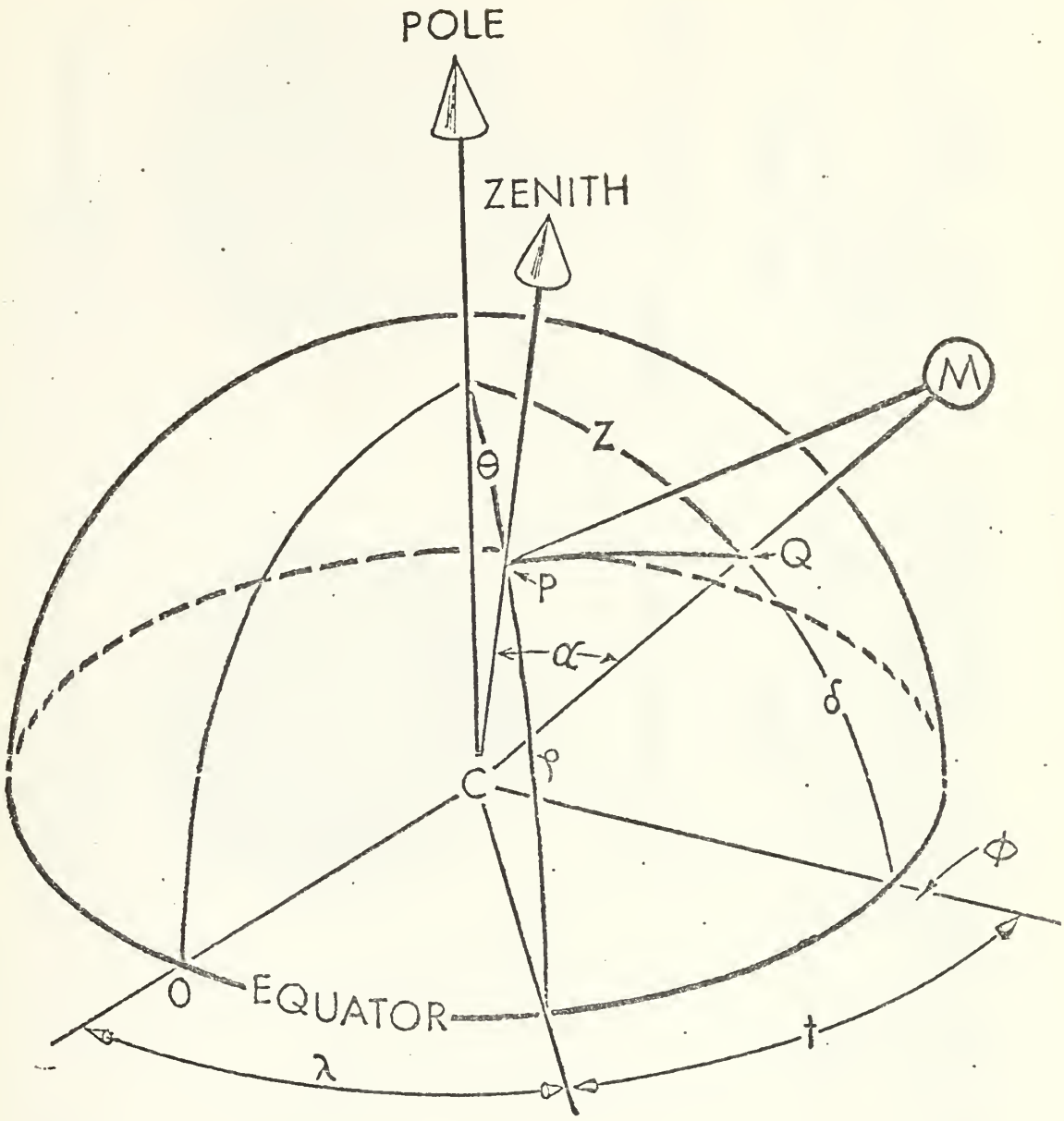

Figure 6. Geometric Relation between Station Coordinates and Tide Producing Body Angular Coordinates. Where α is the zenith angle of the tide producing body at the station location P. P is at colatitude φ and longitude λ. Z is the polar angle and ϑ the terrestrial east longitude of M. (Adopted from Munk and Cartwright)

$$W_n = GM \cdot \frac{r^2}{R^3} \sum_{n=2}^{N} (r/R)^{n-2} P_n(Z)$$

$$.98\, W_n \approx W_2 = GM \frac{r^2}{R^3} P_2(Z) = GM \frac{r^2}{R^3}\left(\frac{3}{2}\cos^2 Z - \frac{1}{2}\right) = GM \frac{r^2}{R^3}(S+T+Z)$$

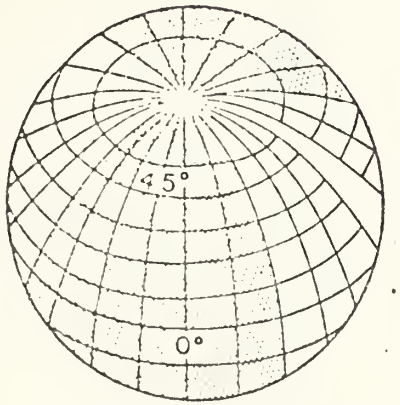

SECTORIAL

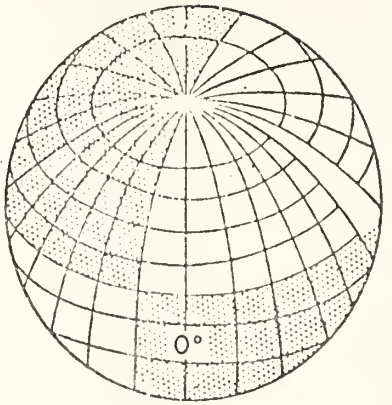

TESSERAL

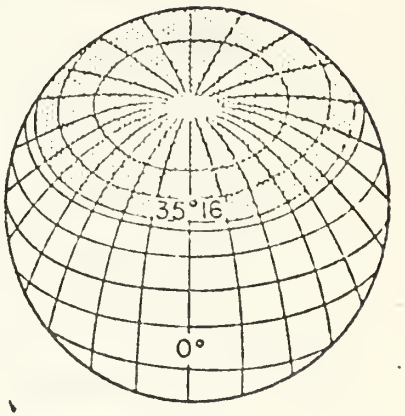

ZONAL

$\cos^2\varphi \cos^2\delta \cos 2H$ | $\sin 2\varphi \sin 2\delta \cos H$ | $3(\sin^2\varphi - 1/3)(\sin^2\delta - 1/3)$

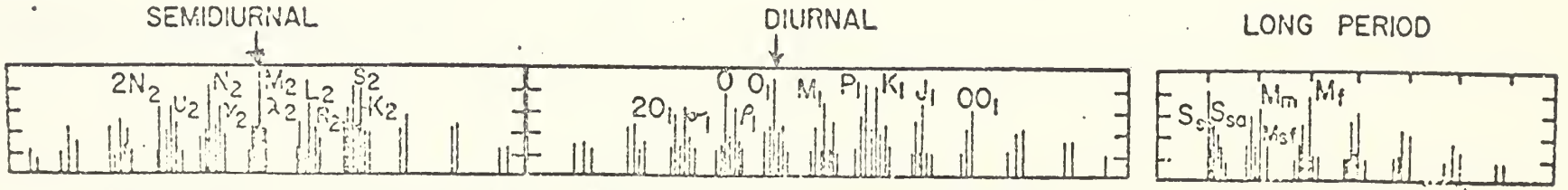

Figure 7. AMPLITUDE SPECTRA AND GEOMETRICAL CHARACTERISTICS OF EARTH TIDES
(Adopted from Melchior [1])

TABLE V. TIDAL CONSTITUENTS USED IN ANALYSIS

Classification	Symbol	Amplitude Coefficient (microgals)	Frequency (deg/solar day)	Wave Description
Diurnal	K_1	+53.050	15.041	Luni-Solar Declinational Wave
	O_1	+37.689	13.943	Lunar Declinational Wave
	P_1	+17.554	14.958	Solar Declinational Wave
	Q_1	+ 7.216	13.398	Lunar Elliptic Wave of O_1
Semi-Diurnal	M_2	+90.812	28.984	Lunar Wave-Circular Orbit
	S_2	+42.286	30.000	Solar Wave-Circular Orbit
	N_2	+17.387	28.439	Lunar Elliptic Wave of M_2
	K_2	+11.506	30.082	Luni-Solar Declinational Wave
Quarter-Diurnal	M_4	-	57.968	Shallow-Water Lunar Wave

(Adopted from Melchior [1])

LIST OF REFERENCES

1. Melchior, P.J., The Earth Tides, Pergamon, 1966.

2. Farrell, W. E., "Deformation of the Earth by Surface Loads," Review of Geophysics and Space Physics, v. 10, No. 3, pp. 761-797, August 1972.

3. Foos, Robert C., Modeling an Input-Output Geokinetic System Utilizing a Finite Element Approach, M.S. Thesis, United States Naval Postgraduate School, Monterey, California, March 1975.

4. Kuo, J.T., Jachens, R.C., Ewing, M., and White, G., "Transcontinental Gravity Profile Across the United States," Science, v. 168, pp. 968-971, 1970.

5. Rosa, Dieter Mayer, "Travel Time Analysis and Distance of Earthquakes Along the Calaveras Fault Zone, California, " Bulletin of the Seismological Society of America, v. 63, No. 2, pp. 713-730, April 1973.

6. Wood, M.D., The Influence of Ocean Tidal Loading on Solid Earth Tides and Tilts in the San Francisco Bay Region, California, Ph.D Thesis, Stanford University, 1969.

7. Wood, M. D., unpublished sources.

8. Wyman, B.D., The Use of Ocean Tide Records to Detect Motion Premonitory to a Tectonic Event in the Long Beach, California Area, M.S. Thesis, Naval Postgraduate School, Monterey, California, 1972.

9. Alterman, L. E., and Kuo, J. T., "Oscillations of the Earth," Proceedings of the Royal Society of London, v. 20, pp. 286-300, 1964.

10. Harrison, J. C., and others, "Earth Tide Observations Made During the International Geophysical Year," Journal of Geophysical Research, v. 68, pp. 1497-1516, 1963.

11. Munk, W. H., and Cartwright, D.E., "Tidal Spectroscopy and Prediction," Philosophical Transactions of the Royal Society (of London), v. 259, pp. 533-581, 1966.

12. Fitzpatrick, Philip M., Principles of Celestial Mechanics, Academic Press, 1970.

13. Harrison, J.C., New Computer Programs for the Calculation of Earth Tides, University of Colorado, November, 1971.

BIBLIOGRAPHY

1. Alterman, L. E., and Kuo, J.T., "Oscillations of the Earth," Proceedings of the Royal Society of London, v. 20, pp. 286-300, 1964.

2. Anderson, D. L., "The San Andreas Fault," Scientific American, v. 225, pp. 53-68, November 1971.

3. Chang, Chien-Wu, Single Channel Prediction for Earth Tidal Tilt Data, M.S. Thesis, United States Naval Postgraduate School, Monterey, California, March 1975.

4. Farrell, W. E., "Deformation of the Earth by Surface Loads," Review of Geophysics and Space Physics, v. 10, No. 3, pp. 761-797, August 1972.

5. Fitzpatrick, Philip M., Principles of Celestial Mechanics, Academic Press, 1970.

6. Foos, Robert C., Modeling an Input-Output Geokinetic System Utilizing a Finite Element Approach, M.S. Thesis, United States Naval Postgraduate School, Monterey, California, March 1975.

7. Harrison, J. C., New Computer Programs for the Calculation of Earth Tides, University of Colorado, November 1971.

8. Harrison, J. C., and others, "Earth Tide Observations Made During the International Geophysical Year," Journal of Geophysical Research, v. 68, pp. 1497-1516, 1963.

9. Kuo, J. T., Jachens, R.C., Ewing, M., and White, G., "Transcontinental Gravity Profile Across the United States," Science, v. 168, pp. 968-971, 1970.

10. Manual of Tide Observations, Publication 30-1, U. S. Department of Commerce, Coast and Geodetic Survey, 1965.

11. Melchior, P. J., The Earth Tides, Pergamon, 1966.

12. Munk, W. H., and Cartwright, D. E., "Tidal Spectroscopy and Prediction," Philosophical Transactions of the Royal Society (of London), v. 259, pp. 533-581, 1966.

13. Rosa, Dieter Mayer, "Travel Time Analysis and Distance of Earthquakes Along the Calaveras Fault Zone, California, " Bulletin of the Seismological Society of America, v. 63, No. 2, pp. 713-730, April 1973.

14. Smith, S. W., and Jungels, P., "Phase Delay of the Solid Earth Tide," Phys. Earth Planet. Interiors 2, pp. 233-238, 1970.

15. Wood, M.D., The Influence of Ocean Tidal Loading on Solid Earth Tides and Tilts in the San Francisco Bay Region, California, Ph.D Thesis, Stanford University, 1969.

16. Wood, M.D., unpublished sources.

17. Wyman, B.D., The Use of Ocean Tide Records to Detect Motions Premonitory to a Tectonic Event in the Long Beach, California Area, M.S. Thesis, United States Naval Postgraduate School, Monterey, California, 1972.

INITIAL DISTRIBUTION LIST

	No. Copies
1. Defense Documentation Center Cameron Station Alexandria, Virginia 22314	2
2. Library, Code 0212 Naval Postgraduate School Monterey, California 93940	2
3. Department Chairman, Code 52 Department of Electrical Engineering Naval Postgraduate School Monterey, California 93940	2
4. U. S. Army Military Personnel Center Attn: DAPC-OPD-II-CS 200 Stovall Street Alexandria, Virginia 22332	2
5. Chief of Naval Personnel Attn: Pers-11b Department of the Navy Washington, D. C. 20370	1
6. Assoc. Professor Donald R. Barr, Code 55Bn Department of Operations Research and Administrative Sciences Naval Postgraduate School Monterey, California 93940	1
7. Assoc. Professor Rex H. Shudde, Code 55Su Department of Operations Research and Administrative Sciences Naval Postgraduate School Monterey, California 93940	1
8. Dr. M. D. Wood United States Geological Survey National Center for Earthquake Research 345 Middlefield Road Menlo Park, California 94025	1
9. CPT Robert L. Keller, USA (Student) 6033 Oakwood Cincinnati, Ohio 45224	1